

Density Wave -Supersolid and Mott Insulator-Superfluid transition in presence of an artificial gauge field : a strong coupling perturbation approach

Rashi Sachdeva, Sankalpa Ghosh

Department of Physics, Indian Institute of Technology, Delhi, New Delhi-110016

(Dated: October 20, 2018)

We study the effect of an artificial gauge field on the zero temperature phase diagram of extended Bose Hubbard model, that describes ultra cold atoms in optical lattices with long range interaction using strong coupling perturbation theory . We determine analytically the effect of the artificial gauge field on the density wave - supersolid (DW-SS) and the the Mott insulator-superfluid (MI-SF) transition boundary . The momentum distribution at these two transition boundaries is also calculated in this approach. It is shown that such momentum distribution which can be observed in time of flight measurement, reveals the symmetry of the gauge potential through the formation of magnetic Brillouin zone and clearly distinguishes between the DW-SS and MI-SF boundary. We also point out that in symmetric gauge the momentum distribution structure at these transition boundaries bears distinctive signatures of vortices in supersolid and superfluid phases.

PACS numbers: 03.75.Lm, 64.70.Tg, 67.80.bd

I. INTRODUCTION

The extended Bose Hubbard Model (eBHM) incorporates the effect of long-range interaction upto various orders by adding the interaction terms between bosons localized at different lattice sites and has been widely studied [1–9]. Recently a number of ultra cold atomic systems has been suggested as possible candidates to realize such models. This includes condensate of ultracold dipolar atoms like ^{52}Cr [10], heteronuclear polar molecules [11] and Rydberg excited ultra cold atomic condensate [12]. The effect of long range interaction can be minimally taken care of by adding a nearest neighbour interactions (NNI) in addition to onsite interactions to the prototype Bose Hubbard (BH) model [13]. The interest in this model stems from the appearance of new phases, namely the Density Wave (DW) phase and the Supersolid (SS) phase, apart from the Mott Insulator (MI) and Superfluid (SF) phase. Both DW and MI phases lack phase coherence as the superfluid order parameter vanishes and, both these phases are incompressible with a finite gap in the particle-hole excitation spectrum.

For a system described by eBHM, in the limit where the hopping between neighbouring sites can be neglected in comparison to the onsite interaction, the system admits DW and MI phases alternatingly as the chemical potential increases. As the hopping amplitude is increased in comparison to the onsite interaction and NNI the systems makes a transition from DW to a SS phase or from MI to a SF phase depending on the chemical potential. The DW phase has alternating particle number at each site in contrast to the MI phase which has same number of particles at each site. This characteristic of DW phase is interesting to explore as this checkerboard arrangement continues even when the interactions are reduced, resulting in transition to SS phase prior to a SF phase.

In the SS phase [14–16] the SF and crystalline orders co-exist resulting in the spatial modulation of superfluid density. This SS phase has been first claimed to be ex-

perimentally observed in solid Helium [17], however the interpretation of the experimental results is a matter of continuing debate [18–21]. On the other hand, the cold atomic condensates with long range interactions loaded in an optical lattice can act as a relatively reliable way to confirm the existence of SS phase. Particularly the effect of artificial gauge field, that can be created either by means of rotation [22, 23] or by imprinting motion-dependent laser induced phase on the internal states [24] on such systems, can lead to the formation of vortex states in such supersolid which has distinctive features as compared to the formation of similar vortices in an ordinary superfluid both in terms of critical velocity of superflow [25] as well as profile [26].

One of the most common probing technique to detect the different phases in BH model or eBHM is to study their momentum distribution. The information about the momentum distribution can be directly extracted from time-of-flight (TOF) absorption imaging in the long time limit of the freely expanding atoms released from the trap [27, 28]. The experimental observation of MI-SF transition with ultra cold atoms in optical lattice [29] was based on this idea. In this context in the current work we study the effect of artificial gauge field on insulating DW and MI phases and their respective transition to SS and SF phases using a strong coupling perturbation approach. We analytically calculate the modification of phase boundaries due to the gauge field, momentum distribution and its gauge potential dependence. We also compare the momentum distribution of the vortex states carrying definite quasi angular momentum at the the DW-SS and MI-SF boundary.

The effect of gauge field on the MI-SF transition in BH model has been studied extensively in recent times both within mean field approximation [30–36] and also by going beyond mean field description [37–40]. Study of frustrated Bose-Hubbard model in presence of staggered fluxes using exact numerical diagonalization was also carried out recently and the dependence of the time

of flight image on the gauge potential was discussed [41]. In comparison, the DW - SS transition in eBHM in presence of a finite flux due to the gauge field [26] as well as in presence of a staggered flux [42] is still in very early stage and was carried out only in mean field framework.

The strong coupling perturbation expansion which we adopt here to study the eBHM model treats the hopping as perturbation [43–45] (for an alternative way of doing strong coupling expansion see [46]) and results from such approach matches quite well with results from quantum monte carlo simulation [47]. Particularly momentum distribution which can be compared with the experimental result of time of flight (TOF) imaging [48, 49] can be calculated using strong coupling approach even in the presence of an artificial gauge field where methods like quantum monte carlo is rather difficult to implement.

The remainder of the paper is organized as follows. In section II, we present the model Hamiltonian and the formalism of our calculations using the strong coupling perturbation theory. In section III, we present the analytical expressions for the phase boundaries between the incompressible (DW and MI) phases and compressible (SS and SF) phases, in presence of artificial gauge field. Section IV includes the calculation of momentum distribution in presence of artificial gauge field obtained by using wave function calculated by strong coupling perturbation theory expansion and also, the quasi angular momentum distribution of the states. A brief summary of the conclusions is presented in section V and the other details of the perturbation calculations are provided in Appendix A and B

II. EXTENDED BOSE HUBBARD MODEL IN PRESENCE OF MAGNETIC FIELD

To describe the effect of nearest neighbour interaction on ultra cold atomic condensate loaded in a square optical lattice in the presence of uniform artificial magnetic field in transverse direction, we introduce the following extended Bose Hubbard Hamiltonian.

$$H = - \sum_{i,j} t_{ij} \hat{b}_i^\dagger \hat{b}_j + \frac{1}{2} \sum_i \hat{n}_i (\hat{n}_i - 1) - \mu \sum_i \hat{n}_i + V \sum_{i,j} \hat{n}_i \hat{n}_j \quad (1)$$

The first term gives us the nearest neighbour hopping where the hopping matrix elements are non zero only for nearest neighbours and is given by $t_{ij} = t e^{i\phi_{ij}}$ with $\phi_{ij} = \int_{r_j}^{r_i} \mathbf{dr} \cdot \mathbf{A}(\mathbf{r})$ and $\mathbf{A}(\mathbf{r})$ is the vector potential corresponding to the artificial gauge field. Here, \hat{b}_i^\dagger , \hat{b}_i and \hat{n}_i are the boson creation, annihilation and number operators respectively. Here, V is the strength of nearest neighbour interaction that minimally captures the effect of long range interaction, μ is the chemical potential. We have rescaled the Hamiltonian by U and thus, all parameters are measured in units of U . We neglect the effect of an overall trap potential assuming that it is sufficiently

shallow and is neutralized by the effect of centrifugal force particularly at the central region of the condensate. We are particularly interested in the limit when $Vd < U/2$, where d is the dimension of the system which is 2 in the present case. In this limit, the alternating sites of the lattice in the DW phase contains n_0 and $n_0 - 1$ particles and such a phase is called $n_0 - \frac{1}{2}$ DW phase. Along the $t = 0$ axis the system will form alternative sequence of $n_0 - \frac{1}{2}$ DW phases followed by MI phases of n_0 particles at each site. In the rest of the paper that the alternative sites of DW phase have population n_A and n_B and finally set $n_A = n_0$ and $n_B = n_0 - 1$ to obtain the corresponding results for $n_0 - \frac{1}{2}$ DW phase.

A. Formalism

Within the frame work of the strong coupling perturbative expansion we calculate the ground-state energy $E_{DW}(n_A, n_B)$ and $E_{MI}(n_0)$ of the DW phase with n_A and n_B bosons on alternating lattice sites, and of the MI phase with $n_A = n_0$ bosons on each lattice site, respectively. We also calculate the energies of the DW particle-hole excitations and MI particle-hole excitations (states with an extra particle or hole), $E_{DW}^{par}(n_A, n_B)$, $E_{DW}^{hol}(n_A, n_B)$, and $E_{MI}^{par}(n_0)$, $E_{MI}^{hol}(n_0)$, respectively. The unperturbed system corresponds to the case ($t = 0$). In this limit, ground state energy as well as the particle hole excitation energy can be analytically determined. Using the Rayleigh-Schrodinger perturbative expansion the ground state energy of DW and MI phases as well the energy of particle hole like excitations over these ground state is calculated in various orders of scaled hopping parameter t .

Both the DW and MI states are gapped since the energy to create a single particle-hole excitations is finite. With increasing t this gap energy starts decreasing. At the critical hopping parameter $t = t_c$ the energy to create a particle-hole pair vanishes and DW phase becomes degenerate with its particle and hole excited state. This gives the value of t at which DW-SS transition takes place. Thus, the phase boundary between the Density Wave and the Supersolid phase is determined by :

$$E_{DW}(n_A, n_B) = E_{DW}^{par/hol}(n_A, n_B) \quad (2)$$

Similarly, the phase boundary between the Mott Insulator phase and the Superfluid phase is determined as :

$$E_{MI}(n_0) = E_{MI}^{par/hol}(n_0) \quad (3)$$

These conditions determine the particle and hole branches of both the insulating lobes (DW and MI), giving us μ^{par} and μ^{hol} as functions of t, V, n_A, n_B (for DW phase) or t, V, n_0 (for MI phase).

B. Wave functions at zeroth order in t

In this section we shall define the ground state wave functions for the DW and MI phases after setting the scaled hopping amplitude $t = 0$ for hamiltonian defined in (1). In this limit these wavefunctions are determined by the competition between interaction energies alone and can be found out exactly. The wave functions for the particle and hole excited states above these ground states will also be mentioned both for DW and MI phase and we shall particularly emphasize the degeneracy associated with such excited states in the $t \rightarrow 0$ limit.

For the DW state, we divide the lattice into sublattices A and B , where each site in sublattice A contains n_A particles and each site in sublattice B contains n_B particles. For $t = 0$, DW wave function can be written as :

$$|\Psi_{DW}^{(0)}\rangle = \prod_{i \in A, j \in B}^{M/2} \frac{(\hat{b}_i^\dagger)^{n_A}}{\sqrt{n_A!}} \frac{(\hat{b}_j^\dagger)^{n_B}}{\sqrt{n_B!}} |0\rangle \quad (4)$$

where M is the total number of lattice sites, and $|0\rangle$ is the state with no particle. Here $\hat{b}_{i,j}^\dagger$ refer to boson creation operator on A and B sublattices, respectively. Since we are interested in calculating the wave function as well as energy of such a state for finite t as a perturbative expansion in the parameter t , the wavefunction defined in (4) is also the wavefunction at the zeroth order of this perturbative expansion.

Unlike the ground state wave function defined in (4), the wave functions for the DW states with an extra particle or hole for $t = 0$ is degenerate. This is because when an extra particle or hole is added to the system, it can go to any of the M lattice sites. However in the case of a DW state, the alternating sites belong to A and B sublattice and contain different number of particles. In the present case $n_A = n_0$ and $n_B = n_0 - 1$. Therefore a particle state over the DW ground state will consist of one particle added to any of site in sublattice B , which contains less number of particle in the ground state. All such states as well their linear combination are degenerate for $t = 0$. Since the total number of sites in B sublattice is $\frac{M}{2}$, therefore the dimension of this degenerate subspace of the one particle excitation is also $\frac{M}{2}$. For the single hole type of excitation over the DW ground state similarly the hole can be created in any site that belongs to sublattice A , containing higher number of particle in the ground state. Therefore the dimension of the degenerate subspace of single hole like excitation is also $\frac{M}{2}$. Because of this degeneracy, to find out the states and energies of particle and hole like excitation for finite t as perturbative expansion in t we need to use the degenerate perturbation theory.

To use degenerate perturbation theory to find out the wave function as well as the energy for particle or hole like excited state, we need to diagonalize the perturbation hamiltonian. To do this we write H given in (1) as

$$H = H_0 + H_P \quad (5)$$

The unperturbed part,

$$H_0 = \frac{1}{2} \sum_i \hat{n}_i(\hat{n}_i - 1) - \mu \sum_i \hat{n}_i + V \sum_{i,j} \hat{n}_i \hat{n}_j \quad (6)$$

and the perturbed part, which is the kinetic energy (hopping) term.

$$H_P = - \sum_{i,j} t_{ij} \hat{b}_i^\dagger \hat{b}_j \quad (7)$$

Now if we diagonalize H_P in the degenerate subspace of either particle or hole like excitation over the DW ground state, we shall find that the degeneracy is only lifted when we include the second order (next nearest neighbour) hopping processes. This is because, each site in sublattice $A(B)$ has only the sites of sublattice $B(A)$ as its neighbour. Thus all the matrix element related by the first order hopping is 0 and we need to go upto the second order to lift the degeneracy. Here we briefly mention the methodology.

To find out the particle and hole excited state which will break the degeneracy when the perturbation is included we write it as a linear superposition of the degenerate basis states, namely

$$|\Psi_{DW}^{par(0)}\rangle = \frac{1}{\sqrt{n_B + 1}} \sum_{j \in B}^{M/2} f_j^{DWB} \hat{b}_j^\dagger |\Psi_{DW}^{(0)}\rangle \quad (8)$$

$$|\Psi_{DW}^{hol(0)}\rangle = \frac{1}{\sqrt{n_A}} \sum_{i \in A}^{M/2} f_i^{DWA} \hat{b}_i |\Psi_{DW}^{(0)}\rangle \quad (9)$$

The correct choice for f_j and f_i will be obtained by diagonalizing the second order perturbation due to the hopping matrix t_{ij} and identifying the corresponding minimum eigenvalue. Therefore f_j^{DWB} will be the eigenvector of $\sum_i t_{ji} t_{ij'}$ with the minimum eigenvalue ($\epsilon^2 t^2$) such that $\sum_{i,j'} t_{ji} t_{ij'} f_{j'}^{DWB} = \epsilon^2 t^2 f_j^{DWB}$ and f_i^{DWA} will be the eigenvector of $\sum_j t_{ij} t_{ji'}$ with the minimum eigenvalue ($\epsilon^2 t^2$) such that $\sum_{j,i'} t_{ij} t_{ji'} f_{i'}^{DWA} = \epsilon^2 t^2 f_i^{DWA}$. The normalization condition also requires that $\sum_{j \in B}^{M/2} |f_j^{DWB}|^2 = 1$ and $\sum_{i \in A}^{M/2} |f_i^{DWA}|^2 = 1$.

Similarly for the MI phase, the non degenerate ground state wave function for $t = 0$ is given by:

$$|\Psi_{MI}^{(0)}\rangle = \prod_{k=1}^M \frac{(\hat{b}_k^\dagger)^{n_0}}{\sqrt{n_0!}} |0\rangle \quad (10)$$

where the index k refers to all the lattice sites. Here also, for $t = 0$ the single particle or hole like excited states over this non-degenerate ground state is degenerate and dimension of these degenerate subspace is M , the total number of lattice sites. Since all sites are equivalent, this degeneracy is lifted in the first order correction of the degenerate perturbation theory, namely when the nearest neighbour hopping is included, unlike the previous case

in DW phase, where to lift the degeneracy one needs to include the next nearest neighbour hopping. Here very briefly we define the details.

The single particle and hole excited state wave functions that will break the degeneracy for finite t is written as

$$|\Psi_{MI}^{par(0)}\rangle = \frac{1}{\sqrt{n_0+1}} \sum_{k=1}^M f_k^{MI} \hat{b}_k^\dagger |\Psi_{MI}^{(0)}\rangle \quad (11)$$

$$|\Psi_{MI}^{hol(0)}\rangle = \frac{1}{\sqrt{n_0}} \sum_{k=1}^M f_k^{MI} \hat{b}_k |\Psi_{MI}^{(0)}\rangle \quad (12)$$

The correct choice of the f_k will be obtained by diagonalizing the first order perturbation due to hopping and locating the minimum eigenvalue state. Thus f_k^{MI} is the eigenvector of the hopping matrix $t_{kk'}$ with the minimum eigenvalue (ϵt)

It may be noted that the H_P is same as the Harper hamiltonian whose spectrum is given by the Hofstadter butterfly. Therefore finding the solution that corresponds to the minimal eigenvalue of the hopping matrix t_{ij} is identical to finding the band minimum in the Hofstadter problem and to locate their corresponding eigenstates. In the following section we shall provide the analytical expression of the perturbatively calculated energy of the

ground state and the particle-hole excitation at finite t and evaluate the phase boundary of the DW-SS transition and the MI-SF transition from this result.

III. ANALYTIC EXPRESSIONS FOR THE MODIFICATION OF PHASE BOUNDARIES

Using many body version of the Rayleigh-Schroedinger perturbation theory the ground state energy of the insulating phases (DW or MI) as well as the energies of the particle or hole like excitation can be expressed as a power series in the scaled hopping amplitude t

$$E(t) = t^0 E_n^{(0)} + t^1 E_n^{(1)} + t^2 E_n^{(2)} + t^3 E_n^{(3)} + \dots \quad (13)$$

where $E_n^{(0)}$ is the energy in the limit $t = 0$, and $tE_n^{(1)}$, $t^2 E_n^{(2)}$ and $t^3 E_n^{(3)}$ are the first order, second order and third order corrections to energy. In the following we present such calculation upto the third order in t and the other details associated with the calculation are relegated to the Appendix A

The expression of the ground state energy of the DW wave state per site is given as

$$\frac{E_{DW}^{ins}}{M} = \left[\frac{1}{2}(n_0 - 1)^2 + zV \frac{n_0(n_0 - 1)}{2} - \mu \frac{2n_0 - 1}{2} \right] - z \left[\frac{n_0^2}{V(z+1)} + \frac{n_0^2 - 1}{2 - V(z+1)} \right] t^2 + O(t^4) \quad (14)$$

In the above expression $z = 2d$ is the co-ordination number of given lattice site which is in the case of a square lattice 4. The first term is the ground state energy at $t = 0$ and the second term is the second order correction due to finite t . Both the first and third order cor-

rection vanishes, We now calculate the energies of the states with an extra particle or hole using Eqs.(8) and (9) in the framework of degenerate perturbation theory. For the particle excited DW states,

$$\begin{aligned} E_{DW}^p &= E_{DW}^{ins} + t^0[(n_0 - 1) + zVn_0 - \mu] \\ &+ t^2 \left[-\frac{n_0(n_0 + 1)\epsilon^2}{(1 - zV)} + \frac{n_0^2\epsilon^2}{((z - 1)V)} + \frac{(n_0^2 - 1)\epsilon^2}{(2 - (z + 1)V)} - \frac{n_0(n_0 + 1)z}{(1 + (z - 2)V)} \right. \\ &\left. - \frac{(n_0^2 - 1)(\epsilon^2 - z)}{(2 - zV)} + \frac{2n_0^2(\epsilon^2 - z)}{((z - 2)V)} \right] + O(t^4) \end{aligned} \quad (15)$$

Comparing this expression with Eq. 13 we find that the first and third order correction vanishes. In a similar

manner the energy of the hole excited DW states can be found out. This turns out to be

$$\begin{aligned}
E_{DW}^h &= E_{DW}^{ins} + t^0[-(1+zV)(n_0-1) + \mu] \\
&+ t^2\left[-\frac{n_0(n_0-1)\epsilon^2}{(1-zV)} + \frac{n_0^2\epsilon^2}{((z-1)V)} - \frac{(n_0^2-1)\epsilon^2}{(2-(z+1)V)}\right. \\
&\left. + \frac{n_0(n_0-1)z}{V(1+(z-2)V)} - \frac{(n_0^2-1)(\epsilon^2-z)}{V(2-zV)} + \frac{2n_0^2(\epsilon^2-z)}{(1+(z-2)V)}\right] + O(t^4)
\end{aligned} \tag{16}$$

In a similar way, the expression for energy of the MI phase and a single particle or hole excitation over it as

perturbative expansion in the scaled hopping parameter t upto third order is given by

$$\frac{E_{MI}^{ins}}{M} = \frac{1}{2}n_0(n_0-1) - \mu n_0 + zV\frac{n_0^2}{2} - zt^2\frac{n_0(n_0+1)}{(1-V)} + O(t^4) \tag{17}$$

$$\begin{aligned}
E_{MI}^p &= E_{MI}^{ins} + t^0[n_0 + zVn_0 - \mu] \\
&- t^1(n_0+1)\epsilon + t^2[n_0(n_0+1)\left[(z-\epsilon^2) + \frac{2(z-\epsilon^2)}{(1-2V)} + \frac{2\epsilon^2}{(1-V)}\right] - n_0(n_0+2)\frac{z}{2(1-V)}] \\
&+ t^3[-n_0(n_0+1)n_0\left[(z-2\epsilon)\epsilon + \frac{(\epsilon^2-3z+3)\epsilon}{(1-V)^2}\right] \\
&- n_0(n_0+1)(n_0+1)\left[(z-\epsilon^2)\epsilon - \frac{(2\epsilon^2-6z+6)\epsilon}{(1-V)^2} + \frac{2\epsilon(z-\epsilon^2)}{(1-2V)^2} + \frac{2\epsilon(\epsilon^2-3z+3)}{(1-V)} + \frac{4(z-2)\epsilon}{(1-2V)} + \frac{4\epsilon(\epsilon^2-3z+3)}{(1-V)(1-2V)}\right] \\
&- n_0(n_0+1)(n_0+1)\frac{4\epsilon(\epsilon^2-3z+3)}{(U-V)(U-2V)} - n_0(n_0+1)(n_0+2)\left[\frac{\epsilon(z-1)}{(1-V)} - \frac{z\epsilon}{4(1-V)^2}\right]] + O(t^4)
\end{aligned} \tag{18}$$

$$\begin{aligned}
E_{MI}^h &= E_{MI}^{ins} + t^0(-(n_0-1) - zVn_0 + \mu) \\
&- t[n_0\epsilon] + t^2[(n_0+1)n_0\left[(z-\epsilon^2) + \frac{2(z-\epsilon^2)}{(1-2V)} + \frac{2\epsilon^2}{(1-V)}\right] - (n_0+1)(n_0-1)\frac{z}{2(1-V)}] \\
&t^3[-n_0(n_0+1)(n_0+1)\left[(z-2\epsilon)\epsilon + \frac{(\epsilon^2-3z+3)\epsilon}{(1-V)^2}\right] \\
&- n_0(n_0+1)n_0\left[(z-\epsilon^2)\epsilon - \frac{(2\epsilon^2-6z+6)\epsilon}{(1-V)^2} + \frac{2\epsilon(z-\epsilon^2)}{(1-2V)^2} + \frac{2\epsilon(\epsilon^2-3z+3)}{(1-V)} + \frac{4(z-2)\epsilon}{(1-2V)} + \frac{4\epsilon(\epsilon^2-3z+3)}{(1-V)(1-2V)}\right] \\
&- n_0(n_0+1)(n_0+1)\frac{4\epsilon(\epsilon^2-3z+3)}{(U-V)(U-2V)} - n_0(n_0+1)(n_0-1)\left[\frac{\epsilon(z-1)}{(1-V)} - \frac{z\epsilon}{4(1-V)^2}\right]] + O(t^4)
\end{aligned} \tag{19}$$

It may be seen that unlike in the case of DW phase, for the MI phase the the perturbative correction to the energy for finite t appears in the first order term itself and the second and third order corrections that appear in Eq.(18) and (19) is comparatively much smaller in magnitude. However we still kept the calculation upto the same order so that the entire phase diagram which comprises of DW as well as MI phase is given within the same order of the perturbation theory. In the following sections, using from the above expressions of energy of the ground state and their corresponding particle hole excitation we shall

determine the MI-SF and DW-SS phase boundary from the relations (2) and (3).

A. Determination of the DW-SS and MI-SF boundary from the strong coupling expansion

Fig. (1) represents the phase diagram of the first four insulating lobes for the eBHM in two dimension (square lattice) in presence of artificial magnetic field. It shows the increasing stability of the insulating phase i.e the DW

and MI phases grows in size as the strength of magnetic field is increased from zero to finite values. This is due to the localizing effect of magnetic field on the moving bosons, thus favouring the insulating phases to occupy a larger area in the phase diagram.

The minimum eigen value ϵ used in calculation of energy expressions, involves the diagonalization of the hopping matrix, which is gauge dependent. The location of the minimum eigen value ϵ depends on the choice of the gauge potential, while the eigen value itself is not. We consider a rational flux $\nu = p/q$ and calculate the minimum eigen values of the hopping matrix t_{ij} following [50]. The shape of the insulating lobes for the Mott phase is different from the DW phase, as observed in Fig (1) in two dimensions. This is because, the Mott states with an extra particle or hole, have corrections to first order in t , while the DW states have corrections to second order in t . So, as $t \rightarrow 0$, the slope of the Mott state will be finite, while it will vanish for the DW lobes. Hence, the shapes of the two insulating lobes are always different. Moreover, the shapes of the insulating lobes depend on the dimensionality of the system and also, on the application of artificial magnetic field [37]. The mean field theories always give a concave shape to the MI and DW lobes[26] as the dimensionality only enters as a prefactor in the expression for μ as a function of t , while the strong coupling expansion easily distinguishes the shape of insulating lobes in different dimensions and also, in presence of artificial magnetic field. The determination of these transition boundary using strong coupling perturbation theory is one of the main results in this paper, Since the transition at the boundary in this model belongs to the universality class of $2 + 1$ dimensional XY model, the critical exponents can also be found out through an expansion of the chemical potential. This was done in [45] and we shall not discuss this issue further.

In the next section, we calculate the effect of artificial magnetic field on the momentum distribution of the insulating phases (DW and MI), with both gauge choices, Landau gauge and symmetric gauge.

IV. CALCULATION OF MOMENTUM DISTRIBUTION

The standard experimental way of probing the properties of an ultra cold atomic condensate is through TOF absorption imaging of the freely expanding atoms released from the trap [28]. Same method is used for probing the condensate loaded in optical lattice as well. The quantity that is measured experimentally in such TOF expansion is the momentum distribution of this ultra cold atomic ensembles. In this section we shall first provide the method of calculation of the momentum distribution within the framework of strong coupling expansion. Subsequently we provide our results and their analysis. We shall particularly show that in the presence of an artificial magnetic field the TOF image actually depends on the

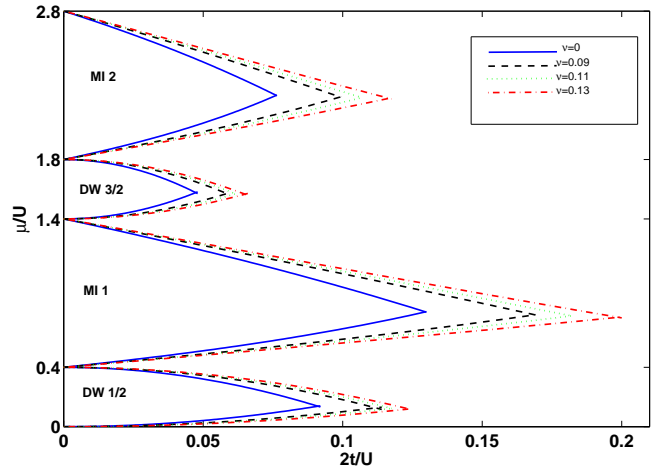


FIG. 1: (Color Online) Phase diagram for the eBHM in presence of artificial magnetic field for $Vd/U=0.2$. The effect of increasing magnetic field is to increase the stability of the DW and MI lobes

means to produce effective magnetic field. As already mentioned in all these discussion we have not taken into account the existence of an overall trap potential assuming it to shallow. Thus the discussion we present can be related to the bulk region of trapped condensate where the effect of the trap potential can be neglected.

The momentum distribution $n(\mathbf{k})$ is defined as the Fourier transform of the one body density matrix, $\rho(\mathbf{r}, \mathbf{r}') = \langle \psi^\dagger(\mathbf{r})\psi(\mathbf{r}') \rangle$, [52]. Therefore,

$$n(\mathbf{k}) = \int d\mathbf{r} \int d\mathbf{r}' \rho(\mathbf{r}, \mathbf{r}') e^{i\mathbf{k} \cdot (\mathbf{r} - \mathbf{r}')} \quad (20)$$

where $\psi^\dagger(\mathbf{r})$ and $\psi(\mathbf{r})$ are the bosonic field operators at the position \mathbf{r} , respectively, and \mathbf{k} is the momentum. The expectation value is taken in the many-body ground state and the corresponding wave function is determined using strong coupling perturbation theory as a power series in scaled hopping amplitude t (in the unit of U).

To evaluate (20) we expand the field operators in the basis set of Wannier functions, such that

$$\psi(\mathbf{r}) = \frac{1}{\sqrt{M}} \sum_l w(\mathbf{r} - \mathbf{R}_l) b_l$$

where M is the total number of lattice sites, $w(\mathbf{r} - \mathbf{R}_l)$ is the Wannier function localized at site l with position \mathbf{R}_l and b_l is the boson annihilation operator. Consequently, the momentum distribution becomes

$$n(\mathbf{k}) = \frac{1}{M} \sum_{l,l'} w^*(\mathbf{k}_l) w(\mathbf{k}_{l'}) \langle b_l^\dagger b_{l'} \rangle e^{i\mathbf{k} \cdot (\mathbf{R}_l - \mathbf{R}_{l'})} \quad (21)$$

where $w(\mathbf{k}) = \int d\mathbf{r} w(\mathbf{r}) e^{i\mathbf{k}\cdot\mathbf{r}}$ is the fourier transform of the usual Wannier function $w(\mathbf{r})$. The summation indices $l \in \{A, B\}$ and $l' \in \{A, B\}$ includes the entire lattice. The wave functions for the insulating phases are calculated perturbatively upto second order in t which is the first significant order. The higher order correction can be neglected since $t \ll 1$, Upto second order, the wave function for the insulating state (MI/DW) can then be written as

$$|\psi_{ins}\rangle = |\Psi_{ins}^{(0)}\rangle + |\Psi_{ins}^{(1)}\rangle + |\Psi_{ins}^{(2)}\rangle + O(t^3) \quad (22)$$

Here, $|\Psi_{ins}^0\rangle = |\Psi_{MI/DW}^{(0)}\rangle$ defined in (4) and (10) and

$$|\Psi_{ins}^{(1)}\rangle = \sum_{m \neq |\Psi_{ins}^{(0)}\rangle} \frac{\langle m | H_P | \Psi_{ins}^{(0)} \rangle}{E_{0m}} |m\rangle \quad (23)$$

$$|\Psi_{ins}^{(2)}\rangle = \sum_{m, m' \neq |\Psi_{ins}^{(0)}\rangle} \frac{\langle m' | H_P | m \rangle \langle m | H_P | \Psi_{ins}^{(0)} \rangle}{E_{0m'} E_{0m}} |m'\rangle \quad (24)$$

In the expression for the first order correction (23), the matrix element of H_P (hopping matrix) is taken between the first-order intermediate (excited) state $|m\rangle$ and the zeroth-order state defined in (4) and (10), where as $|m'\rangle$ in the expression of the second order correction (24) is the second order intermediate (excited) state. Also, $E_{0m} = E_0 - E_m$ is the energy difference between the first order intermediate state $|m\rangle$ and zeroth order state $|\Psi_{ins}^{(0)}\rangle$ and $E_{0m'} = E_0 - E_{m'}$ is the energy difference between the second order intermediate state $|m'\rangle$ and zeroth order state $|\Psi_{ins}^{(0)}\rangle$

To elucidate the meaning of the above terms appearing at the various orders of the perturbation theory, we depict the first and second order hopping processes respectively in Fig. (2) and Fig. (3) for the simplest case of a 2×2 square lattice unit cell. In the diagram given in Fig. (2) (a), we depict the ground state wave function for the DW state for $t = 0$ for this unit cell whose wave function is can be written as

$$|\Psi_{DW}^{(0)}\rangle = |n_A^{(1)}, n_B^{(2)}, n_A^{(3)}, n_B^{(4)}\rangle \quad (25)$$

Here the superscript (i) correspond to the location of a given lattice site. All the subsequent diagrams in the same figure (Fig.2(b)-(i)) depict all the possible $|m\rangle$ state defined in (23) which is connected to the DW ground state in Fig. 2(a) by a single hopping. For example, the state depicted in Fig. (2) correspond to $|m\rangle = |n_A^{(1)} + 1, n_B^{(2)} - 1, n_A^{(3)}, n_B^{(4)}\rangle$. The matrix element of H_P between this state and the ground state can be calculated as

$$\frac{\langle m | H_P | \Psi_{ins}^{(0)} \rangle}{E_{0m}} = \frac{-\sqrt{n_B(n_A + 1)}t_{12}}{(-2 + (z + 1)V)}$$

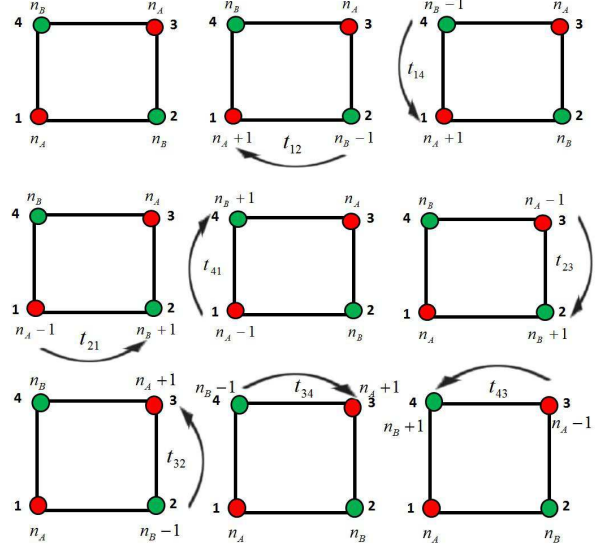


FIG. 2: (Color Online) Possibilities for the first order intermediate (excited) state for the DW phase in a 2×2 lattice. The figure (a) corresponds to the ground state wave function in the limit $t = 0$

and contribute to the first order corrections in the expression (23). The further details of these calculations are given in the Appendix B.

Next, we calculate the second order correction to the wave function of the DW state (eq 24). For every first order intermediate state $|m\rangle$, there will be number of possible second order intermediate states. For example, for the just discussed $|m\rangle = |n_A^{(1)} + 1, n_B^{(2)} - 1, n_A^{(3)}, n_B^{(4)}\rangle$ (Fig.2(b)) which is connected to the ground state by single hopping, the corresponding possibilities for $|m'\rangle$ are shown in Fig. (3) (a)-(g) which is seven in number.

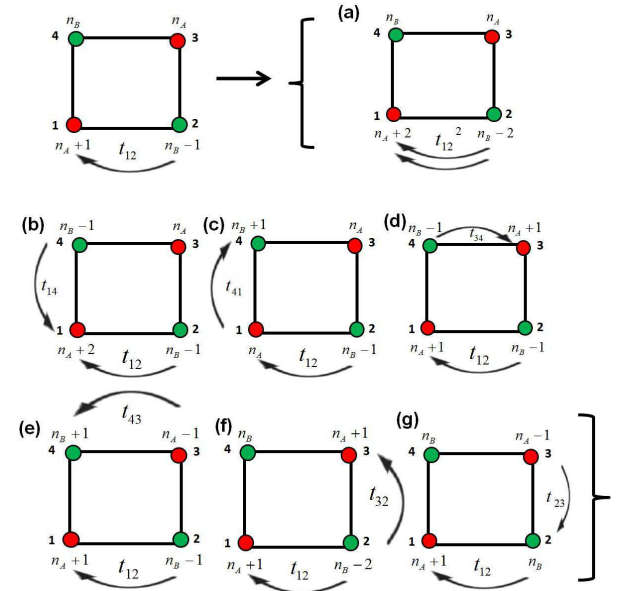


FIG. 3: (Color Online) Second order intermediate states for $|m\rangle = |n_A^{(1)} + 1, n_B^{(2)} - 1, n_A^{(3)}, n_B^{(4)}\rangle$ (the first diagram)

In the same way, for each possible first order intermediate (excited) state $|m\rangle$ (Fig. 2(b)-(i)), the second order excited states are calculated and thus by adding all possible combinations, the second order correction to wave function is determined (Eq. 24). The details of the calculation is provided in Appendix B.

With the help of above expressions for perturbation

$$\begin{aligned}
n_{DW}(\mathbf{k}) &= \frac{2n_0 - 1}{2} - \left[\frac{n_0^2}{(z-1)V} + \frac{(n_0^2 - 1)}{2 - (z+1)V} \right] \epsilon(\mathbf{k}) \\
&+ 2n_0 \left[\frac{n_0^2}{2(z-1)^2 V^2} + \frac{(n_0^2 - 1)}{2[2 - (z+1)V]^2} + \frac{n_0^2}{(z-1)V} + \frac{(n_0^2 - 1)}{[2 - (z+1)V]} \right] [\epsilon^2(\mathbf{k}) - 2dt^2] \\
&+ O(t^3)
\end{aligned} \tag{26}$$

Similarly, for the MI phase with n_0 particles on each lattice site, the momentum distribution in presence of gauge field is

$$\begin{aligned}
n_{Mott}(\mathbf{k}) &= n_0 - \frac{2n_0(n_0 + 1)}{1 - V} \epsilon(\mathbf{k}) + n_0(n_0 + 1)(2n_0 + 1) \\
&\times (\epsilon^2(\mathbf{k}) - 2dt^2) \frac{3 - 2V}{(1 - V)^2} + O(t^3)
\end{aligned} \tag{27}$$

In either of the above expression of momentum distribution (26) and (27), the dispersion $\epsilon(\mathbf{k})$ is the minimum eigenvalue of the artificial magnetic flux dependent hopping matrix T or t_{ij} multiplied by a pre-factor $\frac{2}{M}$ for DW phase and $\frac{1}{M}$ for the MI phase where M is the total number of sites along a given direction. The matrix T in the lattice site basis can be written

$$T = \begin{bmatrix} t_{11} & t_{12} & t_{13} & \dots & t_{1M} \\ t_{21} & \dots & t_{ij} & \dots & \\ \vdots & \vdots & \vdots & \vdots & \vdots \\ t_{m1} & \dots & & t_{M,M-1} & t_{MM} \end{bmatrix} \tag{28}$$

As described in (1), $t_{ij} = te^{i\phi_{ij}}$ is the gauge dependent hopping amplitude from site i to site j and non-vanishing only if i and j are nearest neighbours. Through $\phi_{ij} = \int_{r_j}^{r_i} d\mathbf{r} \cdot \mathbf{A}(\mathbf{r})$ this hopping amplitude explicitly depend on the gauge potential with $A(\mathbf{r})$ as the vector potential. In the next sub section, we provide the results for the effect of artificial magnetic field on the momentum distribution of the DW and MI phases.

A. Effect of the presence of gauge field on the momentum distribution

The effect of artificial gauge field on the on the MI-SF and DW-SS transition boundary have distinctive features which can be demonstrated by plotting the momentum

corrections, the DW ground state wave function can be determined upto the second order in perturbation theory using the general expression (22) and subsequently normalized within the same order of perturbation theory. Substituting of this wavefunction in the expression (21) for momentum distribution yields th $n(\mathbf{k})$ for the DW phase as

distribution derived in (26) and (27) in the $k_x - k_y$ plane at these transition boundaries. Since the matrix T in (28) explicitly depends on the gauge potential, the momentum distribution reflects in itself the gauge potential structure.

To demonstrate this we calculate the dispersion $\epsilon(\mathbf{k})$ for two types of artificial gauge fields on the system, the Landau gauge and the Symmetric gauge and evaluate the corresponding momentum distribution structure. The vector potential in Landau (L) and Symmetric (S) gauge are respectively given as

$$\mathbf{A}^L(\mathbf{r}) = \mathbf{B}(0, x, 0) = 2\pi\nu x\hat{y} \tag{29}$$

$$\mathbf{A}^S(\mathbf{r}) = \mathbf{B}(-y, x, 0) = \pi\nu(x\hat{y} - y\hat{x}) \tag{30}$$

where we consider that the flux due to the corresponding gauge field through the unit shell $\nu = p/q$ is rational.

In the Landau gauge \mathbf{A}^L , following [50] we denote the co-ordinate of a site i on the square lattice by pair of integers $\{m, n\}$ in the unit of the lattice spacing a . For Landau gauge potential therefore the phase of the hopping parameter $\phi_{ij} = 0$ is if the link along x direction ($i \rightarrow j = \{m, n\} \rightarrow \{m+1, n\}$) and $\phi_{ij} = 2\pi n\nu$ if the link is along the y direction such ($i \rightarrow j = \{m, n\} \rightarrow \{m, n+1\}$). In terms of these notations the eigenvalue equation $T\psi = \epsilon\psi$ on the lattice can be written as

$$\begin{aligned}
&-t[\psi_{n+1,m} + \psi_{n-1,m} + \\
&e^{2\pi i\nu n}\psi_{n,m+1} + e^{-2\pi i\nu n}\psi_{n,m-1}] = \epsilon\psi_{n,m}
\end{aligned} \tag{31}$$

The lattice wavefunctions that appears in Eq. (31) can be obtained by operating $\psi_{n,m}$ by magnetic translation operator. Such operators are given as $T_{\mathbf{R}} = \exp(\frac{i}{\hbar} \mathbf{R} \cdot [\mathbf{p} + \frac{\hbar}{m} \mathbf{A}(\mathbf{r})])$ [51] where R is the lattice translational vector and it is known the operators along the x and y axis do not commute since $\hat{T}_{a\hat{x}}\hat{T}_{a\hat{y}}\hat{T}_{a\hat{x}}^{-1}\hat{T}_{a\hat{y}}^{-1} = \exp(2\pi i\nu)$. In case of Landau gauge and for $\nu = \frac{p}{q}$ the required commutator is given by $[T_{qa\hat{x}}, T_{a\hat{y}}] = 0$. To ensure that the wave function remain single valued at a given lattice

point as an unit cell is traversed, the enlarged unit cell known as magnetic unit cell therefore has $q \times 1$ sites. as compared to the unit cell in the absence of such magnetic field. Correspondingly the Brillouin Zone (BZ) is reduced with $-\pi \leq k_y \leq \pi, -\pi/q \leq k_x \leq \pi/q$ and is called the magnetic Brillouin zone (MBZ). As we shall see the momentum distribution $n(\mathbf{k})$ shows the formation of such MBZ.

Since $[T, \hat{p}_y] = 0$ in the Landau gauge the wave function $\psi_{n,m}(k_x, k_y) = e^{ik_y m} e^{ik_x n} \phi_n(k_x, k_y)$ where $k_{x,y}$ are the components of the Bloch wave vectors. Substituting this expression in the eigenvalue equation (31) one gets the following one dimensional eigenvalue equation

$$-t[e^{ik_x} \phi_{n+1} + e^{-ik_x} \phi_{n-1} + 2 \cos(k_y + 2\pi\nu n) \phi_n] = \epsilon \phi_n \quad (32)$$

The eigenvalues $\epsilon(\mathbf{k})$ now can be determined from the condition

$$\det \begin{bmatrix} M_1 & e^{-ik_x} & 0 & \dots & e^{ik_x} \\ e^{ik_x} & M_2 & \dots & \dots & \\ 0 & \vdots & \vdots & \vdots & 0 \\ \dots & \dots & & M_{q-1} & e^{-ik_x} \\ N_q & & 0 & e^{ik_x} & M_q \end{bmatrix} = 0 \quad (33)$$

with $M_n = 2\cos(k_y a + 2\pi n \phi) - \epsilon(\mathbf{k})$ and, where $n = 0, 1, \dots, q-1$. The eigenvalue matrix is $q \times q$ dimensional because of the q times enhancement of the magnetic unit cell. And its minimum eigenvalue $\epsilon(\mathbf{k})$ is q -fold degenerate since $\epsilon(k_x, k_y) = \epsilon(k_x, k_y + \frac{2\pi\alpha}{q})$ where $\alpha = 0, \dots, (q-1)$. Each of this minimum will correspond to a peak in the momentum distribution which is calculated using (26) and (27). This has been plotted in Fig 4(a) and (b) for MI and DW phase.

Thus in the Landau gauge potential, in MI phase one gets q peaks in $n(\mathbf{k})$ at $(k_x, k_y) = (0, \frac{2\pi n}{q})$, with $n = 0, 1, \dots, q-1$. Accordingly Fig 4(a) shows the momentum distribution for $q = 4$ which has peaks at $(0, 0)$, $(0, \pm\pi/2)$ and $(0, \pm\pi)$. For the DW phase, $\nu = 1/q$ with $q = 4$, we again get peaks at $n(\mathbf{k})$ at $(0, 0)$, $(0, \pm\pi/2)$ and $(0, \pm\pi)$, but in addition, there also exists small peaks at the corners of the reduced BZ, as shown in fig 4(b). The appearance of extra peaks at the BZ corners distinguishes DW phase from the MI phase. Since the DW phase consists of two interpenetrating sublattices A and B , even in the absence of any applied magnetic field, the BZ structure of the DW phase has double periodicity whereas the usual MI state has a single periodicity. This results in appearance of small extra peaks in the momentum distribution of DW even in the absence of magnetic field [49]. Upon application of magnetic field, we observe small peaks in the DW momentum distribution at the BZ corners, which is again attributed to the reduced periodicity of the DW phase compared to MI phase.

When one uses a symmetric gauge potential given in (30) the commuting magnetic translation operators

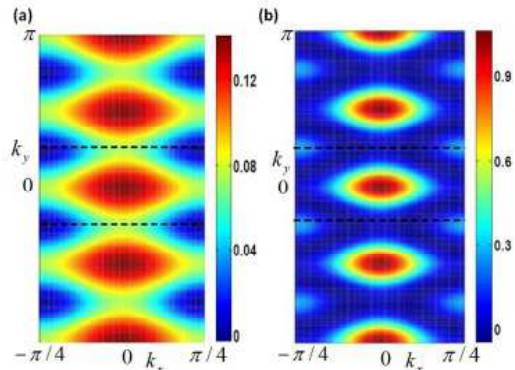


FIG. 4: (Color Online) Momentum distribution for the (a) MI and (b) DW phase in landau gauge potential for $\nu = \frac{1}{4}$, plotted in the reduced brillouin zone $-\pi \leq k_x \leq \pi$ and $-\pi/4 \leq k_y \leq \pi/4$

are $\hat{T}_{2qa\hat{x}}$ and $\hat{T}_{2qa\hat{y}}$. The corresponding discretized eigenvalue equation was discussed in detail in [26]. Following the preceding discussion it can be shown that the magnetic unit shell should be $2q \times 2q$ of the unit cell in the absence field. The factor 2 comes because the phase accumulated when one goes around an unit cell in the square lattice is $\pi i \nu$ in presence of the gauge potential (30). Accordingly the MBZ will be defined as $(-\frac{\pi}{2q} \leq k_x \leq \frac{\pi}{2q}, -\frac{\pi}{2q} \leq k_y \leq \frac{\pi}{2q})$. This results in the formation of peaks in momentum distribution at $(\pm\pi n/q, \pm\pi n/q)$. The momentum distribution of the MI phase in presence of symmetric gauge potential, for rational flux $\nu = 1/4$ is shown in fig 5(a). The peak in the momentum distribution is observed at the center $((0, 0))$ and smaller peaks are seen at the corners in the range $(-\pi/4 \leq k_x \leq \pi/4, -\pi/4 \leq k_y \leq \pi/4)$. Same calculation for the DW phase, in a symmetric gauge potential, shows the existence small peaks at the BZ (doubly reduced) corners, in addition to the peak at $(0, 0)$, as shown in fig 5(b).

The effect of application of symmetric gauge potential to the system is equivalent to rotating the system [26, 33] and thus, leads to formation of vortices in the system when the superfluid order parameter is finite. Since we perform our calculations at the phase boundary, the results for the momentum distribution of the DW and MI phases in presence of symmetric gauge potential, provides information about the structure of vortex in a supersolid (at the DW-SS phase boundary) and vortex in a superfluid (at the MI-SF phase boundary). The preceding discussion demonstrates that rotating supersolid reflects some extra peaks in the momentum distribution in addition to the peaks observed in a rotating ordinary superfluid. These extra peaks are clearly demonstrated in fig (6) and is one of the central result of this work.

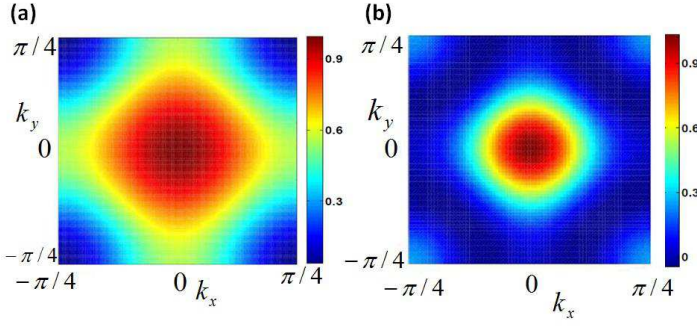


FIG. 5: (*Color Online*) Momentum distribution for the (a) MI and (b) DW phase in symmetric gauge potential for $\nu=1/4$, plotted in the range $-\pi/4 \leq k_x \leq \pi/4$ and $-\pi/4 \leq k_y \leq \pi/4$

Since momentum distribution can be measured us-

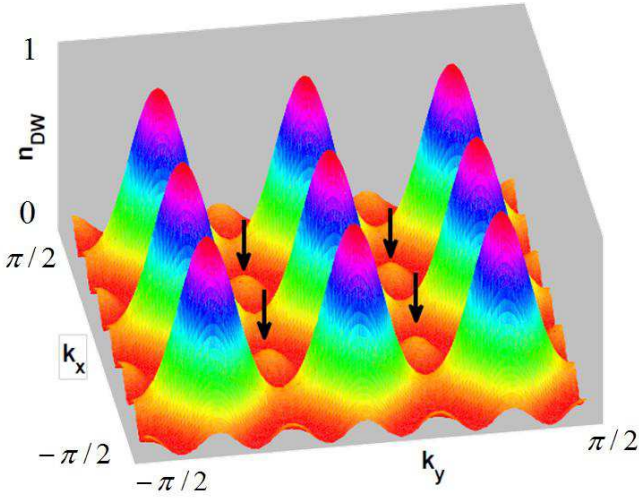


FIG. 6: (*Color Online*) Extra small peaks in the DW momentum distribution $n(\mathbf{k})$ symmetric gauge potential. The arrows show the location of the extra peaks at intermediate points

ing TOF absorption imaging technique, this provides a way to experimentally distinguish between the super-solid phase and superfluid phase by comparing the respective vortex profile. To analyze this issue further in the next section we compare the momentum distribution $n(\mathbf{k})$ in symmetric gauge to the momentum distribution corresponding to the many body states having definite quasi-angular momentum in a symmetric gauge potential. This quasi-angular momentum are analogues of the Bloch-momentum, but for a rotationally invariant system and has been discussed in detail [53]

B. Quasi-angular momentum distribution

In this section we re evaluate the momentum distribution $n(\mathbf{k})$ but for a fixed quasi angular momentum and compare this with $n(\mathbf{k})$ demonstrated in Fig. 5.

To simplify calculation we approximate the wannier functions as delta functions to calculate the correlation function with a fixed value of angular momentum given to the system. The field operators can now be expanded as

$$\psi(\mathbf{r}) = \frac{1}{\sqrt{M}} \sum_l e^{i2\pi m l/M} \delta(\mathbf{r} - \mathbf{r}_l) b_l \quad (34)$$

where m is the quasi-angular momentum, M is the number of lattice sites. Substituting this in the expression (20) yields

$$n(\mathbf{k}) = \frac{1}{M} \sum_{l,l'} e^{i2\pi m(l-l')/M} \delta^*(\mathbf{r} - \mathbf{r}_l) \delta(\mathbf{r} - \mathbf{r}_{l'}) \times \langle \psi_{ins} | b_l^\dagger b_{l'} | \psi_{ins} \rangle e^{i\mathbf{k} \cdot (\mathbf{r}_l - \mathbf{r}_{l'})} \quad (35)$$

The summation indices $l \in \{A, B\}$ and $l' \in \{A, B\}$ includes the entire lattice.

As compared to the expression (21), in (35) the system has a prefixed value of quasi angular momentum and therefore we can associate a vortex phase with the system.

For DW and MI phase, the quasi angular momentum distribution is given by :

$$n_{DW}(\mathbf{k}) = \frac{1}{M} \sum_{l,l'} e^{i2\pi m(l-l')/M} \delta^*(\mathbf{r} - \mathbf{r}_l) \delta(\mathbf{r} - \mathbf{r}_{l'}) e^{i\mathbf{k} \cdot (\mathbf{r}_l - \mathbf{r}_{l'})} \left(\frac{2n_0 - 1}{2} - \left[\frac{n_0^2}{V(z-1)} + \frac{(n_0^2 - 1)}{2U - V(z+1)} \right] t \right) + 2n_0 \left[\frac{n_0^2}{2V^2(z-1)^2} + \frac{(n_0^2 - 1)}{2[2U - V(z+1)]^2} + \frac{n_0^2}{UV(z-1)} + \frac{(n_0^2 - 1)}{U[2U - V(z+1)]} \right] t^2 + O(t^3)$$

Similar expression for $n(\mathbf{k})$ with a given quasi angular momentum for the MI phase can also be evaluated withing strong coupling expansion. For a square lattice with four sites, Fig. 7 (a) shows the momentum distribution

for $m = 0$ for DW phase. The $m = 0$ state has a peak at $k = 2\pi n$, with n as an integer. However for higher quasi angular momentum state $m=1$, $n(\mathbf{k})$ vanishes at $k = 2\pi n$ in Fig. 7 (b). Again the DW-SS phase boundary can be

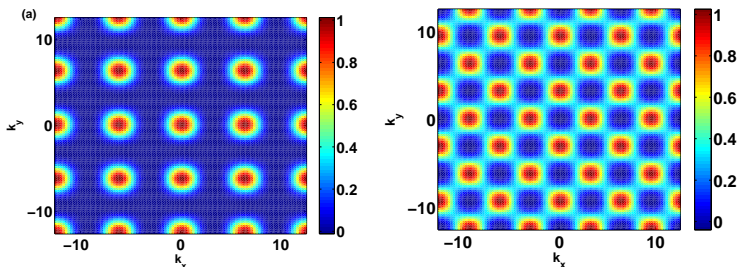


FIG. 7: (*Color Online*) Quasi angular momentum distribution of the DW phase for (a) $m=0$, (b) $m=1$, plotted over a range $-4\pi \leq k_x, k_y \leq 4\pi$

separated from the MI-SF phase boundary by noting the appearance of small extra peaks in the former case. To demonstrate these small peaks clearly we plot the cross sectional plots for the DW phase in Fig. 8.

We also plot the quasi momentum distribution for the state $m = 1$ for MI and DW phases.

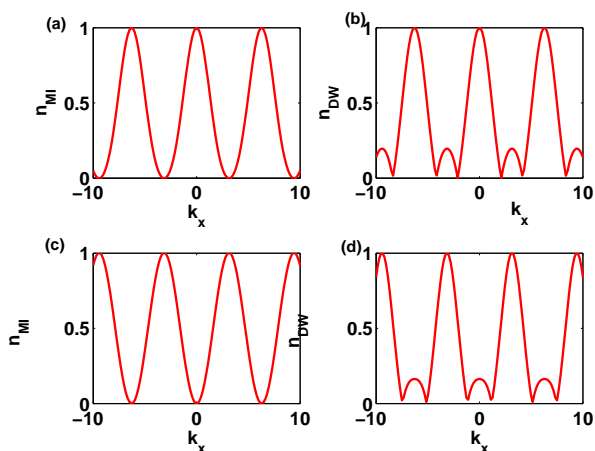


FIG. 8: (*Color Online*) The cross sectional plots for $m=0$ and $m=1$ quasi angular momentum state for MI((a),(c)) and DW ((b), (d)) phases. The DW phase shows distinctive peaks compared to MI phase

Quasi angular momentum is connected with the phase information and hence, the vorticity. The fact that a zero quasi angular momentum state can be distinguished from a non-zero one by looking at the corresponding $n(\mathbf{k})$, allows the experimenters to verify that vorticity has entered in the system through the TOF measurement.

V. SUMMARY AND CONCLUSION

To summarize we have determined the modification of the DW-SS and MI-SF phase boundary corresponding to EBHM at zero temperature due to the effect of an artificial gauge field within the framework of strong

coupling perturbation theory. Using the same approach we calculated the momentum distribution at this phase boundary which can be verified experimentally using the time of flight imaging. The momentum distribution reflects the symmetry of the gauge potential. The momentum distribution shows distinctive feature at the DW-SS phase boundary as compared to the MI-SF phase boundary. Particularly evaluating the momentum distribution for states with definite quasi-angular momentum at such phase boundary in a symmetric gauge we clearly demonstrate how this can be used to probe the vortex profile of the SS phase at the DW-SS boundary due to the action of the gauge field. There have been significant progress in cold atom experiments in identifying the enigmatic supersolid phase in ultra cold atomic systems [54–56]. Our calculation will hopefully augment further study in the behavior of such SS phase in presence of an artificial gauge field.

RS is supported by a fellowship given by CSIR and the work of SG is supported by a grant from Planning section, IIT Delhi.

Appendix A: Perturbation corrections to the ground state and particle hole excitation energy in the DW and MI phases in presence of artificial magnetic field

1. Corrections to ground state energy

Here we provide the detail expressions of $E_n^{(0)}, E_n^{(1)}, E_n^{(2)}, E_n^{(3)}$ that appears in the equation (13) for DW phase. The zeroth order term is given by

$$\begin{aligned} E_{DW}^{(0)} &= \langle \Psi_{DW}^{(0)} | H_0 | \Psi_{DW}^{(0)} \rangle \\ &= M \left(\frac{n_A(n_A - 1) + n_B(n_B - 1)}{4} + zV \frac{n_A n_B}{2} \right. \\ &\quad \left. - \mu \frac{n_A + n_B}{2} \right) \end{aligned} \quad (\text{A1})$$

The first order correction is given as

$$E_{DW}^{(1)} = \langle \Psi_{DW}^{(0)} | H_P | \Psi_{DW}^{(0)} \rangle = 0 \quad (\text{A2})$$

This is because $\langle n_A - 1 | n_A \rangle_i = \langle n_B - 1 | n_B \rangle_j = 0$, where i and j can be any site. For the same reason all odd order correction like $E_n^{(3)}$ also vanishes. The second order correction, which is also the first non-vanishing correction is given by

$$\begin{aligned} E_{DW}^{(2)} &= \sum_{m \neq n} \frac{|\langle \Psi_{DW}(m_A, m_B) | H_P | \Psi_{DW}^{(0)}(n_A, n_B) \rangle|^2}{(E_{n_A, B} - E_{m_A, B})} \\ &= \left[\frac{n_A(n_B + 1)}{(n_A - n_B - 1) + (zn_B - zn_A + 1)V} + \frac{n_B(n_A + 1)}{(n_B - n_A - 1) + (zn_A - zn_B + 1)V} \right] M z t^2 \end{aligned} \quad (\text{A3})$$

Substituting the above expressions in the right hand side of Eq. (13) one gets the ground state energy of the DW

state upto the third order as

$$\begin{aligned} \frac{E_{DW}(n_A, n_B)}{M} &= \frac{n_A(n_A - 1) + n_B(n_B - 1)}{4} + zV \frac{n_A n_B}{2} - \mu \frac{n_A + n_B}{2} \\ &\quad + \left[\frac{n_A(n_B + 1)}{(n_A - n_B - 1) + (zn_B - zn_A + 1)V} + \frac{n_B(n_A + 1)}{(n_B - n_A - 1) + (zn_A - zn_B + 1)V} \right] z t^2 + O(t^4) \end{aligned} \quad (\text{A4})$$

Setting $n_A = n_0$ and $n_B = n_0 - 1$ in the above expression we get the expression (14).

2. Calculation of energy of DW state with an extra particle or hole

Explicitly written wave function of the DW phase with an extra particle is

$$\begin{aligned} |\Psi_{DW}^{par(0)} \rangle &= \sum_{j \in B, j=1}^{M/2} f_j^{DW(B)} |n_A^{(1)}, n_A^{(3)} \dots n_A^{(M/2)}; \\ &\quad n_B^{(2)} \dots n_B^{(j-1)}, n_B^{(j)} + 1 \dots n_B^{(M)} \rangle \end{aligned}$$

Also, we can get the corresponding corrections for the ground state in MI phase by substituting in the above expressions for the DW state $n_A = n_B = n_0$. The ground state energy in the MI Phase given in Eq. (17) can be obtained from the expression (A4) by putting $n_A = n_B = n_0$.

where $f_j^{DW(B)}$ is the eigenvector of $\sum_i t_{ji} t_{ij}'$ with the minimum eigenvalue $(\epsilon^2 t^2) f_j^{DW(B)}$, such that $\sum_{i, j'} t_{ji} t_{ij}' f_{j'}^{DW(B)} = \epsilon^2 t^2 f_j^{DW(B)}$,

The zeroth order energy of the DW phase is

$$\begin{aligned} E_{DW}^{par(0)} &= \langle \Psi_{DW}^{par(0)} | H_0 | \Psi_{DW}^{par(0)} \rangle \\ &= E_{DW}^{(0)} + n_B + zVn_A - \mu \end{aligned} \quad (A5)$$

First order correction in energy

$$\begin{aligned} E_{DW}^{par(1)} &= \langle \Psi_{DW}^{par(0)} | H_P | \Psi_{DW}^{par(0)} \rangle \\ &= 0 \end{aligned} \quad (A6)$$

Again, all odd order terms vanishes. The second order correction to the energy of DW phase with an extra particle is given as

$$\begin{aligned} E_{DW}^{par(2)} &= \sum_{m \neq n} \frac{|\langle \Psi_{DW}^{par}(m_A, m_B) | H_P | \Psi_{DW}^{par(0)}(n_A, n_B) \rangle|^2}{(E_{n_A, B} - E_{m_A, B})} \\ &= E_{DW}^{(1)} + \left[\frac{(n_A + 1)(n_B + 1)\epsilon^2 t^2}{(n_B - n_A) + (zn_A - zn_B)V} - \frac{n_A(n_B + 1)\epsilon^2 t^2}{(n_A - n_B - 1) + (zn_B - zn_A + 1)V} \right] \\ &\quad + \left[-\frac{n_B(n_A + 1)\epsilon^2 t^2}{(n_B - n_A - 1) + (zn_A - zn_B + 1)V} + \frac{n_A(n_B + 2)zt^2}{(n_A - n_B - 2) + (zn_B - zn_A + 2)V} \right] \\ &\quad + \left[\frac{n_B(n_A + 1)(\epsilon^2 - z)t^2}{(n_B - n_A - 1) + (zn_A - zn_B)V} + \frac{2n_A(n_B + 1)(\epsilon^2 - z)t^2}{(n_A - n_B - 1) + (zn_B - zn_A + 2)V} \right] \end{aligned} \quad (A7)$$

Thus, adding equations (A5), (A7) gives us the energy of DW state with an extra particle upto the third order.

In the same way, the energy of the DW phase with an extra hole can be calculated and is given as

$$\begin{aligned} E_{DW}^{hol}(n_A, n_B) &= E_{DW}^{ins}(n_A, n_B) - (n_A - 1) - zVn_B + \mu + \\ &\quad + \left[\frac{n_A n_B \epsilon^2 t^2}{(n_B - n_A) + (zn_A - zn_B)V} - \frac{n_A(n_B + 1)\epsilon^2 t^2}{(n_A - n_B - 1) + (zn_B - zn_A + 1)V} \right] \\ &\quad + \left[-\frac{n_B(n_A + 1)\epsilon^2 t^2}{(n_B - n_A - 1) + (zn_A - zn_B + 1)V} + \frac{(n_A - 1)(n_B + 1)zt^2}{(n_A - n_B - 2) + (zn_B - zn_A + 2)V} \right] \\ &\quad + \left[\frac{n_B(n_A + 1)(\epsilon^2 - z)t^2}{(n_B - n_A - 1) + (zn_A - zn_B)V} + \frac{2n_A(n_B + 1)(\epsilon^2 - z)t^2}{(n_A - n_B - 1) + (zn_B - zn_A + 2)V} \right] + O(t^4) \end{aligned} \quad (A8)$$

Again the expressions (15) and (16) are obtained by substituting $n_A = n_0$ and $n_B = n_0 - 1$.

where the coefficient f_j are to be determined from the lowest eigenvalue $\sum_{j'} t_{jj'} f_j^{MI} = zt f_j^{MI}$ as explained earlier. The zeroth order correction to the energy of MI phase with an extra particle is now given as

3. Calculation of energy of MI state with an extra particle or hole

The MI phase with an extra particle has the following wave function,

$$|\Psi_{MI}^{par(0)}\rangle = \sum_{j=1}^M f_j^{MI} |n_0^{(1)}, n_0^{(2)} \dots n_0^{(j)} + 1, \dots n_0^{(M)}\rangle$$

$$\begin{aligned} E_{MI}^{par(0)} &= \langle \Psi_{MI}^{par(0)} | H_0 | \Psi_{MI}^{par(0)} \rangle \\ &= E_{MI}^{(0)} + n_0 + zVn_0 - \mu \end{aligned} \quad (A9)$$

The first order correction to the energy of this state is

$$E_{MI}^{par(1)} = \langle \Psi_{MI}^{par(0)} | H_P | \Psi_{MI}^{par(0)} \rangle = -(n_0 + 1)\epsilon t \quad (A10)$$

The second order energy correction for the extra particle MI phase is as calculated below

$$\begin{aligned}
E_{MI}^{par(2)} &= \sum_{m \neq n} \frac{|\langle \Psi_{MI}^{par}(m_0) | H_P | \Psi_{MI}^{par(0)}(n_0) \rangle|^2}{(E_n^0 - E_m^0)} \\
&= E_{MI}^{(2)} \\
&\quad + n_0(n_0 + 1) \left[(z - \epsilon^2) + \frac{2(z - \epsilon^2)}{(1 - 2V)} + \frac{2\epsilon^2}{(1 - V)} \right] t^2 \\
&\quad - \frac{n_0(n_0 + 2)z}{2(1 - V)} t^2 \tag{A11}
\end{aligned}$$

$$\begin{aligned}
E_{MI}^{par(3)} &= \sum_{k \neq n} \sum_{m \neq n} \frac{\langle \Psi_{MI}^{par(0)}(n_0) | H_P | \Psi_{MI}^{par}(m_0) \rangle \langle \Psi_{MI}^{par}(m_0) | H_P | \Psi_{MI}^{par}(k_0) \rangle \langle \Psi_{MI}^{par}(k_0) | H_P | \Psi_{MI}^{par}(n_0) \rangle}{(E_m^0 - E_n^0)(E_k^0 - E_m^0)} \\
&\quad - \langle \Psi_{MI}^{par(0)}(n_0) | H_P | \Psi_{MI}^{par(0)}(n_0) \rangle \sum_{m \neq n} \frac{|\langle \Psi_{MI}^{par(0)}(n_0) | H_P | \Psi_{MI}^{par}(m_0) \rangle|^2}{(E_m^0 - E_n^0)^2} \\
&= -n_0(n_0 + 1) \left\{ n_0 \left[(z - 2\epsilon)\epsilon + \frac{(\epsilon^2 - 3z + 3)\epsilon}{(1 - V)^2} \right] \right\} t^3 \\
&\quad - n_0(n_0 + 1) \left\{ (n_0 + 1) \left[(z - \epsilon^2)\epsilon - \frac{(2\epsilon^2 - 6z + 6)\epsilon}{(1 - V)^2} + \frac{2\epsilon(z - \epsilon^2)}{(1 - 2V)^2} + \frac{2\epsilon(\epsilon^2 - 3z + 3)}{(1 - V)} + \frac{4(z - 2)\epsilon}{(1 - 2V)} \right] \right\} t^3 \\
&\quad - n_0(n_0 + 1)(n_0 + 1) \frac{4\epsilon(\epsilon^2 - 3z + 3)}{(1 - V)(1 - 2V)} t^3 - n_0(n_0 + 1)(n_0 + 2) \left[\frac{\epsilon(z - 1)}{(1 - V)} - \frac{z\epsilon}{4(1 - V)^2} \right] t^3 \tag{A12}
\end{aligned}$$

Adding Eqs. (A9), (A10), (A11) and (A12) gives the energy expression for MI phase with an extra particle given in (18). This expression recovers the known result of onsite Bose Hubbard model when $V = 0$ [43].

The energy for the Mott phase with an extra hole is calculated, in the same way as above and is given in eq (19).

plicity). We apply perturbation theory on $|\Psi_{DW}^{(0)}\rangle$ to calculate $|\Psi_{DW}^{ins}\rangle$ up to the desired order eq(22). Using the diagrams given in Fig. (2), the 1st order correction to the ground state wave function of DW state in for a unit cell in a square lattice (for all possible $|m\rangle$'s) can be explicitly written as

Appendix B: Perturbative correction to the wave function and momentum distribution

1. Corrections to the wave function for the insulating DW phase

We start with the definition of the ground state wave function for the DW phase eq(25) (2x2 lattice, for sim-

$$\begin{aligned}
|\Psi_{DW}^{(1)}\rangle &= \sum_{m \neq |\Psi_{DW}^{(0)}\rangle} \frac{-\sum_{l'} t_{l'} \langle m | b_l^\dagger b_{l'} | 0 \rangle}{E_{0m}} |m\rangle \\
&= \frac{-\sqrt{n_B(n_A+1)}}{E_1} [t_{12} |n_A^{(1)} + 1, n_B^{(2)} - 1, n_A^{(3)}, n_B^{(4)}\rangle + t_{14} |n_A^{(1)} + 1, n_B^{(2)}, n_A^{(3)}, n_B^{(4)} - 1\rangle \\
&\quad + t_{32} |n_A^{(1)}, n_B^{(2)} - 1, n_A^{(3)} + 1, n_B^{(4)}\rangle + t_{34} |n_A^{(1)}, n_B^{(2)}, n_A^{(3)} + 1, n_B^{(4)} - 1\rangle] \\
&\quad - \frac{\sqrt{n_A(n_B+1)}}{E_2} [t_{21} |n_A^{(1)} - 1, n_B^{(2)} + 1, n_A^{(3)}, n_B^{(4)}\rangle + t_{23} |n_A^{(1)}, n_B^{(2)} + 1, n_A^{(3)} - 1, n_B^{(4)}\rangle \\
&\quad + t_{41} |n_A^{(1)} - 1, n_B^{(2)}, n_A^{(3)}, n_B^{(4)} + 1\rangle + t_{43} |n_A^{(1)}, n_B^{(2)}, n_A^{(3)} - 1, n_B^{(4)} + 1\rangle]
\end{aligned} \tag{B1}$$

where

$$\begin{aligned}
E_1 &= (n_B - n_A - 1) + (zn_A - zn_B + 1)V \\
E_2 &= (n_A - n_B - 1) + (zn_B - zn_A + 1)V
\end{aligned}$$

To calculate the second order correction using eq(24) following Fig. (3) we consider $|m\rangle = |n_A^{(1)} + 1, n_B^{(2)} + 1, n_A^{(3)}, n_B^{(4)}\rangle$

$$\frac{\langle m | H_P | 0 \rangle}{E_{0m}} = \frac{-\sqrt{n_B(n_A+1)} t_{12}}{E_1} \tag{B2}$$

The corresponding possibilities for $|m'\rangle$ for $|m\rangle = |n_A^{(1)} + 1, n_B^{(2)} - 1, n_A^{(3)}, n_B^{(4)}\rangle$ are represented in Fig. (3(c)-(i)). For illustration let us choose $|m'\rangle = |n_A^{(1)} + 2, n_B^{(2)} - 2, n_A^{(3)}, n_B^{(4)}\rangle$. Then

$$\begin{aligned}
E_{0m'} &= E_0 - E_{m'} = E_{01} \\
&= 2(n_A - n_B - 2) + (2zn_A - 2zn_B + 4)V
\end{aligned}$$

The contribution of this $|m'\rangle$ state to the second order correction to DW wave function is

$$\begin{aligned}
|\Psi_{DW}^{(2)}\rangle_{a_1} &= \frac{\sqrt{n_B(n_A+1)(n_A+2)(n_B-1)}}{(E_1)(E_{01})} t_{12}^2 \\
&\quad |n_A^{(1)} + 2, n_B^{(2)} - 2, n_A^{(3)}, n_B^{(4)}\rangle
\end{aligned}$$

Similarly, we calculate the contribution from all of the $|m'\rangle$ states corresponding to this particular $|m\rangle$. Summing over this contributions we the second order correction to the wave function due to this $|m\rangle$ state which looks like

$$\begin{aligned}
|\Psi_{DW}^{(2)}(|m\rangle)\rangle_a &= \frac{\sqrt{n_B(n_A+1)(n_A+2)(n_B-1)}}{(E_1)(E_{01})} t_{12}^2 |n_A^{(1)} + 2, n_B^{(2)} - 2, n_A^{(3)}, n_B^{(4)}\rangle \\
&\quad + \frac{n_B \sqrt{(n_A+1)(n_A+2)}}{(E_1)(E_{02})} t_{12} t_{14} |n_A^{(1)} + 2, n_B^{(2)} - 1, n_A^{(3)}, n_B^{(4)} - 1\rangle \\
&\quad + \frac{(n_A+1) \sqrt{n_B(n_B+1)}}{(E_1)(E_{03})} t_{12} t_{41} |n_A^{(1)}, n_B^{(2)} - 1, n_A^{(3)}, n_B^{(4)} + 1\rangle \\
&\quad + \frac{(n_A+1) \sqrt{n_B(n_B-1)}}{(E_1)(E_{04})} t_{12} t_{32} |n_A^{(1)} + 1, n_B^{(2)} - 2, n_A^{(3)} + 1, n_B^{(4)}\rangle \\
&\quad + \frac{n_B \sqrt{n_A(n_A+1)}}{(E_1)(E_{05})} t_{12} t_{23} |n_A^{(1)} + 1, n_B^{(2)}, n_A^{(3)} - 1, n_B^{(4)}\rangle \\
&\quad + \frac{\sqrt{n_A n_B (n_A+1)(n_B+1)}}{(E_1)(E_{06})} t_{12} t_{43} |n_A^{(1)} + 1, n_B^{(2)} - 1, n_A^{(3)} - 1, n_B^{(4)} + 1\rangle \\
&\quad + \frac{n_B(n_A+1)}{(E_1)(E_{07})} t_{12} t_{34} |n_A^{(1)} + 1, n_B^{(2)} - 1, n_A^{(3)}, n_B^{(4)} - 1\rangle
\end{aligned}$$

Following the same procedure for all other $|m\rangle$ states defined in Fig. (2) and adding all contributions, we get the total second order correction to wave-function for the DW phase. where

2. Terms in momentum distribution calculation

The momentum distribution in (21) can be written as

$$\begin{aligned} n(\mathbf{k}) &= \frac{|W(\mathbf{k})|^2}{M} \sum_{l,l'} \langle \Psi_{DW} | b_l^\dagger b_{l'} | \Psi_{DW} \rangle e^{-i\mathbf{k}\cdot(\mathbf{R}_l - \mathbf{R}_{l'})} \\ &= n(\mathbf{k})^{(0)} + n(\mathbf{k})^{(1)} + n(\mathbf{k})^{(2)} \end{aligned}$$

$$n(\mathbf{k})^{(0)} = \frac{|W(\mathbf{k})|^2}{M} \sum_{l,l'} \{ \langle \Psi_{DW}^{(0)} | b_l^\dagger b_{l'} | \Psi_{DW}^{(0)} \rangle \} e^{-i\mathbf{k}\cdot(\mathbf{R}_l - \mathbf{R}_{l'})} \quad (\text{B3})$$

$$\begin{aligned} n(\mathbf{k})^{(1)} &= \frac{|W(\mathbf{k})|^2}{M} \sum_{l,l'} \{ \langle \Psi_{DW}^{(0)} | b_l^\dagger b_{l'} | \Psi_{DW}^{(1)} \rangle \\ &\quad + \langle \Psi_{DW}^{(1)} | b_l^\dagger b_{l'} | \Psi_{DW}^{(0)} \rangle \} e^{-i\mathbf{k}\cdot(\mathbf{R}_l - \mathbf{R}_{l'})} \end{aligned} \quad (\text{B4})$$

$$\begin{aligned} n(\mathbf{k})^{(2)} &= \frac{|W(\mathbf{k})|^2}{M} \sum_{l,l'} \{ \langle \Psi_{DW}^{(0)} | b_l^\dagger b_{l'} | \Psi_{DW}^{(2)} \rangle \\ &\quad + \langle \Psi_{DW}^{(1)} | b_l^\dagger b_{l'} | \Psi_{DW}^{(1)} \rangle + \langle \Psi_{DW}^{(2)} | b_l^\dagger b_{l'} | \Psi_{DW}^{(0)} \rangle \} \\ &\quad e^{-i\mathbf{k}\cdot(\mathbf{R}_l - \mathbf{R}_{l'})} \end{aligned} \quad (\text{B5})$$

Here we keep terms only upto second order and terms $\langle \Psi_{DW}^{(1)} | b_l^\dagger b_{l'} | \Psi_{DW}^{(2)} \rangle$, $\langle \Psi_{DW}^{(2)} | b_l^\dagger b_{l'} | \Psi_{DW}^{(1)} \rangle$ and $\langle \Psi_{DW}^{(0)} | b_l^\dagger b_{l'} | \Psi_{DW}^{(2)} \rangle$ are neglected. Using the wave function from eq(25) we get

$$n(\mathbf{k})^{(0)} = |W(\mathbf{k})|^2 \left(\frac{n_A + n_B}{2} \right) \quad (\text{B6})$$

$$\begin{aligned} n(\mathbf{k})^{(1)} &= -\frac{n_B(n_A + 1)}{E_1} \frac{|W(\mathbf{k})|^2}{M/2} \sum_{l,l'} t_{ll'} e^{i\mathbf{k}\cdot(\mathbf{R}_l - \mathbf{R}_{l'})} - \frac{n_A(n_B + 1)}{E_2} \frac{|W(\mathbf{k})|^2}{M/2} \sum_{l,l'} t_{ll'} e^{i\mathbf{k}\cdot(\mathbf{R}_l - \mathbf{R}_{l'})} \\ &= |W(\mathbf{k})|^2 \left[\frac{n_B(n_A + 1)}{E_1} + \frac{n_A(n_B + 1)}{E_2} \right] \epsilon(\mathbf{k}) \end{aligned} \quad (\text{B7})$$

and

$$\begin{aligned} n(\mathbf{k})^{(2)} &= \frac{|W(\mathbf{k})|^2}{M/2} \left[\frac{n_B(n_A + 1)}{2E_1^2} + \frac{n_A(n_B + 1)}{2E_2^2} - \frac{n_B(n_A + 1)}{E_1} - \frac{n_A(n_B + 1)}{E_2} \right] \times (n_B + n_A + 1) \left[\sum_{l,l',l''} t_{ll'} t_{l'l''} e^{i\mathbf{k}\cdot(\mathbf{R}_l - \mathbf{R}_{l''})} \right] \\ &= |W(\mathbf{k})|^2 \left[\frac{n_B(n_A + 1)}{2E_1^2} + \frac{n_A(n_B + 1)}{2E_2^2} - \frac{n_B(n_A + 1)}{E_1} - \frac{n_A(n_B + 1)}{E_2} \right] \times (n_B + n_A + 1) (\epsilon^2(\mathbf{k}) - 2dt^2) \end{aligned} \quad (\text{B8})$$

-
- [1] G. G. Batrouni, R. T. Scalettar, G. T. Zimanyi and A. P. Kampf, Phys. Rev. Lett. **74**, 2527 (1995).
- [2] A. V. Otterlo, K. H. Wagenblast, R. Baltin, C. Bruder, R. Fazio and G. Schön, Phys. Rev. B **52**, 16176 (1995).
- [3] T. D. Kuhner, S. R. White, and H. Monien, Phys. Rev. B **61**, 12474 (2000)
- [4] L. Santos, G. V. Shlyapnikov, and M. Lewenstein, Phys. Rev. Lett. **90**, 250403 (2003)
- [5] P. Sengupta, L. P. Pryadko, F. Alet, M. Troyer, and G. Schmid, Phys. Rev. Lett. **94**, 207202 (2005)
- [6] G. G. Batrouni, F. Hebert, and R. T. Scalettar, Phys. Rev. Lett. **97**, 087209 (2006)
- [7] D. L. Kovrizhin, G. V. Pai, and S. Sinha, Europhys. Lett. **72**, 162 (2005)
- [8] R. V. Pai and R. Pandit, Phys. Rev. B **71**, 104508 (2005)
- [9] T. Lahaye et al., Rep. Prog. Phys. **72**, 126401 (2009)
- [10] T. Lahaye *et al.*, Nature (London) **448**, 672 (2007).
- [11] K.-K. Ni *et al.*, Science **322**, 231 (2008).
- [12] N. Henkel, R. Nath and T. Pohl, Phys. Rev. Lett **104**, 195302 (2010).
- [13] D. Jaksch et al., Phys. Rev. Lett., **81**, 3108 (1998) ; M. P.A. Fisher et al., Phys. Rev. B **40**, 546 (1989); K. She-shadri et al., Europhys. Lett. **22**, 257 (1993).
- [14] A. F. Andreev and I. M. Lifshitz, JETP **29**, 1107 (1969).
- [15] A.J. Leggett, Phys. Rev. Lett. **25**, 1543 (1970).
- [16] H. Matsuda and T. Tsuneto, Prog. Theor. Phys. Suppl. **46**, 411 (1970).
- [17] E. Kim and M. H. W Chan, Sciences **305**, 1941 (2004)
- [18] J. D. Reppy, Phys. Rev. Lett. **104** 255301 (2010).
- [19] N. Prokof'ev, Adv. Phys. **56**, 381 (2007)
- [20] P. W. Anderson, W. F. Brinkman, D. A. Huse **310**, 1164 (2005).
- [21] S. Balibar, Nature **464**, 176 (2010).
- [22] K.W. Madison, F. Chevy, W. Wohlleben, and J. Dalibard, Phys. Rev. Lett. **84**, 806 (2000); J. R. Abo-Sheer et al., Science **292**, 476 (2001); P. Engels, I. Coddington, P. C. Haljan, and E. A. Cornell, Phys Rev. Lett. **89**, 100403 (2002).
- [23] S. Tung, V. Schweikhard, and E. A. Cornell, Phys. Rev. Lett. **97**, 240402 (2006); R. A. Williams, S. Al Assam, and C. J. Foot, *ibid.* **104**, 050404 (2010).
- [24] Y.-J. Lin et al., Nature, **462**, 628 (2009); Y. J. Lin, R. L. Compton, A. R. Perry, W. D. Phillips, J. V. Porto, and I. B. Spielman, Phys. Rev. Lett. **102**, 130401 (2009).
- [25] I. Danshita and D. Yamamoto, Phys. Rev. A **82**, 013645 (2010).
- [26] R. Sachdeva, S. Johri and S. Ghosh, Phys. Rev. A **82**, 063617 (2010)
- [27] F. Gerbier *et al.*, Phys. Rev. Lett. **101**, 155303 (2008).
- [28] E. Toth, A. M. Rey, and P. B. Blaike, Phys. Rev. A **78**, 013627(2008).
- [29] M. Greiner et al. Nature **415**, 39 (2002).
- [30] J. W. Reijnders and R. A. Duine, Phys. Rev. Lett. **93**, 060401 (2004)
- [31] R. Bhat, B.M. Peden, B. T. Seaman, M. Kramer, L. D. Carr, and M. J. Holland, Phys. Rev. A **74**, 063606 (2006)
- [32] C. Wu, H. D. Chen, J. P. Hu, and S. C. Zhang, Phys. Rev. A **69**, 043609 (2004)
- [33] D. S. Goldbaum and E. J. Mueller, Phys. Rev. A **77**, 033629 (2008); D. S. Goldbaum, Ph.D. thesis, Cornell University, 2009 (unpublished)
- [34] R. O. Umucalilar and M. O. Oktel, Phys. Rev. A **76**, 055601 (2007); M. O. Oktel, M. Nita, and B. Tanatar Phys Rev. B **75**, 045133 (2007)
- [35] E. Lundh, Europhys. Lett. **84**, 10007 (2008)
- [36] V. W. Scarola and S. Das Sarma, Phys. Rev. Lett. **98**, 210403 (2007)
- [37] M. Niemeier, J. K. Freericks and H. Monien, Phys. Rev. B **60**, 2357 (1999)
- [38] S. Powell, R. Barnett, R. Sensarma, and S. DasSarma, Phys. Rev. Lett. **104**, 255303 (2010)
- [39] S. Powell, R. Barnett, R. Sensarma and S. D. Sarma, Phys. Rev. A **83**, 013612 (2011)
- [40] S. Sinha and K. Sengupta, Europhys. Lett. **93**, 30005 (2011).
- [41] G. Moller and N. R. Cooper, Phys. Rev. A **82**, 063625 (2010).
- [42] O. Tieleman, A. Lazarides and C. Morais Smith, Phys. Rev. A **83**, 013627 (2011)
- [43] J. K. Freericks and H. Monien, Phys. Rev. B **53**, 2691 (1996).
- [44] J. K. Freericks and H. Monien, Europhys. Lett. **26**, 545 (1994)
- [45] M. Iskin and J. K. Freericks, Phys. Rev. A **79**, 053634 (2009)
- [46] K. Sengupta and N. Dupuis, Phys. Rev. A **71**, 033629 (2005).
- [47] W. Krauth, N. Trivedi and D. Ceperley, Phys. Rev. Lett. **67**, 2307 (1991).
- [48] J. K. Freericks *et al.*, Phys. Rev. A **79**, 053631 (2009)
- [49] M. Iskin and J. K. Freericks, Phys. Rev. A **80**, 063610 (2009)
- [50] M. Kohmoto, Phys. Rev. B **39**, 11943 (1989); J. Bellisard, Ch. Krefl and R. Seiler, J. Phys. A **24**, 2239 (1990); Y. Hasegawa, P. Lederer, T. M. Rice and P. B. Wiegmann, Phys. Rev. Lett. **63**, 907 (1989).
- [51] J. Zak, Phys. Rev. **134**, A1602 (1964).
- [52] L.P. Pitaevskii and S. Stringari, *Bose Einstein Condensation*, (Clarendon Press, Oxford, 2003)
- [53] B.M. Peden, R. Bhat, M. Kramer and M. J. Holland, J. Phys. B: At. Mol. Opt. Phys. **40**, 3725 (2007).
- [54] M. Vengalattore, J. Guzman, S. R. Leslie, F. Serwane, and D. M. Stamper-Kurn, Phys. Rev. A **81**, 053612 (2010).
- [55] K. Baumann, C. Guerlin, F. Brennecke, and T. Esslinger, Nature (London) **464**, 1301 (2010).
- [56] S. Gopalakrishnan, B. L. Lev, and P. M. Goldbart, Phys. Rev. A **82**, 043612 (2010)